Eur. Phys. J. Special Topics **171**, 81–90 (2009)

DOI: 10.1140/epjst/e2009-01014-x

THE EUROPEAN PHYSICAL JOURNAL SPECIAL TOPICS

Regular Article

Simulating thermohydrodynamics by finite difference solutions of the Boltzmann equation

R. Surmas[1,a], C.E. Pico Ortiz[1,b], and P.C. Philippi[1,c]

Mechanical Engineering Department, Federal University of Santa Catarina, 88040-900 Florianópolis, SC, Brazil

Abstract. The formulation of a consistent thermohydrodynamics with a discrete model of the Boltzmann equation requires the representation of the velocity moments up to the fourth order. Space-filling discrete sets of velocities with increasing accuracy were obtained using a systematic approach in accordance with a quadrature method based on prescribed abscissas (Philippi et al., Phys. Rev. E, 73 (5), n. 056702, 2006). These sets of velocities are suitable for collision-propagation schemes, where the discrete velocity and physical spaces are coupled and the Courant number is unitary. The space-filling requirement leads to sets of discrete velocities which can be large in thermal models. In this work, although the discrete sets of velocities are also obtained with a quadrature method based on prescribed abscissas, the lattices are not required to be space-filling. This leads to a reduced number of discrete velocities for the same approximation order but requires the use of an alternative numerical scheme. The use of finite difference schemes for the advection term in the continuous Boltzmann equation has shown to have some advantages with respect to the collision-propagation LBM method by freeing the Courant number from its unitary value and reducing the discretization error. In this work, a second order Runge-Kutta method was used for the simulation of the Sod's shock tube problem, the Couette flow and the Lid-driven cavity flow. Boundary conditions without velocity slip and temperature jumps were written for these discrete Boltzmann equation by splitting the velocity distribution function into an equilibrium and a non-equilibrium part. The equilibrium part was set using the local velocity and temperature at the wall and the non-equilibrium part by extrapolating the non-equilibrium moments to the wall sites.

1 Introduction

The lattice Boltzmann (LB) BGK method [1], is a phase space discretization of the Boltzmann equation with a BGK collision operator [2]. In this method, the discretization of the velocity space is coupled with the spatial and temporal discretizations by a unitary Courant number, i.e., the sets of velocities or lattices are space-filling.

In a thermohydrodynamical problem, the mass density, velocity and temperature are the variables of interest. A Chapman-Enskog (CE) analysis shows that, in order to correctly represent the transport of these quantities up to the first order in Knudsen number (Kn), the second, third and fourth order moments of the equilibrium distribution must be exactly retrieved [3]. It can also be shown that when the analysis is performed considering a higher order in Kn, higher order moments are also required to be exactly retrieved [4].

[a] e-mail: surmas@lmpt.ufsc.br
[b] e-mail: capico@lmpt.ufsc.br
[c] e-mail: philippi@lmpt.ufsc.br

The first attempts to discretize this equation in the velocity space had led to LB equations that presented numerical instabilities or deviations from the Navier-Stokes-Fourier equations [3,5,6]. Recently, Philippi et al. (2006) [7], employed a quadrature method based on prescribed abscissas to derive space-filling lattices suitable to LB simulations. These lattices were used to simulate the diffusion of velocity and temperature steps, giving very promising results [8,9].

It was earlier recognized that an increasing in the moment order recovered by the quadrature, which increases often the lattice isotropy, could improve the stability of the algorithm used. Therefore high order isotropic non-space-filling lattices were derived [10,11], with the objective of increasing the algorithm stability. Although these lattices proved to be suitable for thermohydrodynamic problems, there is no formal connection between the equilibrium distribution found in Refs. [10,11] and the continuous Maxwell-Boltzmann equilibrium distribution, see [7]. Furthermore, these lattices are computationally expensive, specially in three dimensional simulations.

An alternative to the LB method to solve the Boltzmann transport equation could be the use of numerical methods based on finite volumes, elements or differences. These options should be considered: a) when the error due to the spatial and time discretizations must be reduced through high order algorithms; b) when adaptative meshes need to be used; c) in simulating mixtures, since, in these cases, the collision-propagation schemes has shown to have quite narrow stability limits [12].

When the spatial-temporal discretization is performed without any coupling with the velocity space discretization, the Courant number becomes free from its unitary value. Although the numerical algorithm often increases in complexity, non-space-filling lattices need a lower number of discrete velocities than space-filling ones.

In this paper, non-space-filling lattices are obtained with the quadrature method based on prescribed abscissas of Philippi et al. (2006). Some of the lattices found are very similar to those cited in [13] and references therein. A second order Runge-Kutta method was applied to the temporal term and the resulting discrete Boltzmann equation was used for the simulation of the Sod's shock tube problem [14], the Couette flow and the Lid-driven cavity flow. Boundary conditions without velocity slip and temperature jumps were written for these discrete Boltzmann equation by splitting the velocity distribution function into an equilibrium and a non-equilibrium part. The equilibrium part was set using the local velocity and temperature on the wall and the non-equilibrium part was set by extrapolating the non-equilibrium moments of the fluid sites to the wall sites.

2 Quadrature based on prescribed abscissas

Considering the Boltzmann transport equation with a BGK collision operator [1], and the following change of variables: $\boldsymbol{x} = L\boldsymbol{x^*}$, $t = Tt^*$, $\boldsymbol{\xi} = l\boldsymbol{\xi^*}/\tau$, where L and T are a characteristic macroscopic length and time, and l e τ are a characteristic microscopic length and time, respectively. The Boltzmann equation becomes:

$$Kn\left(\partial_{t^*} f + \xi^*_\alpha \partial_{\alpha^*} f\right) = f^{eq} - f, \tag{1}$$

where $Kn = l/L \approx \tau/T$ is the Knudsen number (Kn) [15].

Considering the following expansions in the Kn: $f = f^{(0)} + Kn^1 f^{(1)} + Kn^2 f^{(2)} + \ldots$ and $\partial_t = \partial_{t_0} + Kn^1\partial_{t_1} + Kn^2\partial_{t_2} + \ldots$, the Boltzmann equation can be collected in Kn orders leading to an asymptotic CE analysis. At each Kn order, the mass, momentum and energy equations can be obtained by multiplying the resulting equations by 1, ξ^*_α and ${\xi^*}^2$, integrating them in the velocity space and recomposing the time derivative. Although these equations are not easily obtained when the Kn order is high and considering that the CE analysis has its own drawbacks when the Kn increases [15], this analysis can be used to determine the minimal requirements for a proper discretization of the velocity space [4].

It was shown that the necessary condition for the discrete counterparts of the Boltzmann equation to retain its macroscopic features is that the integrals of the equilibrium distribution

are correctly calculated by the following quadrature [4,7],

$$\int f^{eq}\psi(\boldsymbol{\xi})d\boldsymbol{\xi} = \sum_i w_i f_i^{eq}\psi(\boldsymbol{\xi}_i), \tag{2}$$

for all equilibrium moments of interest, $\psi(\boldsymbol{\xi})$. In the above equation w_i is a weight related to the discrete velocity ξ_i. In this manner, when the mass, momentum and energy balances must be accurate up to the Navier-Stokes-Fourier limit, this quadrature must be exact for the moments: 1, ξ_α, $\xi_\alpha\xi_\beta$, $\xi_\alpha\xi_\beta\xi_\gamma$ and $\xi^2\xi_\alpha\xi_\beta$.

Using a reference temperature T_o and expanding the equilibrium distribution function, f^{eq}, and the moments, $\psi(\boldsymbol{\xi})$, in Hermite polinomials, $\mathscr{H}$, the following orthogonality relations are obtained [9],

$$\frac{1}{2\pi}\int e^{-\boldsymbol{\xi}_o^2/2}\mathscr{H}_{r_j}^{(j)}(\boldsymbol{\xi}_o)\mathscr{H}_{r_n}^{(n)}(\boldsymbol{\xi}_o)d\boldsymbol{\xi}_o = \sum_i W_i\mathscr{H}_{r_j}^{(j)}(\boldsymbol{\xi}_{oi})\mathscr{H}_{r_n}^{(n)}(\boldsymbol{\xi}_{oi}). \tag{3}$$

All Hermite polynomials up to the desired moment order must be orthogonal in relation to the discrete product defined by the above equation with weight $W_i = w_i\frac{m}{2\pi kT_o}e^{-\xi_{oi}^2/2}$ and abscissas $\boldsymbol{\xi}_{oi} = \boldsymbol{\xi}_i/\sqrt{kT_o/m}$. Philippi et al. (2006) showed that when a lattice is invariant under $\pi/2$ rotations and reflections about the x and y axis, the preservation of the norm of each Hermite polynomial in the discrete space assure the orthogonality of these polynomials in this space.

In Philippi et al. [7,8], space-filling lattices were obtained by adding space-filling sets of same magnitude velocities one after another, until the quadrature problem had a closed solution up to the sixth order. In the present work, non-space-filling velocity sets were used. The velocity magnitudes and, in some cases, the orientation of each sub-lattice were set as free parameters to be determined a posteriori. For each order of the quadrature equations, this procedure increases the number of unknowns for a given number of equations and enables a closed solution with a smaller number of discrete velocities in the set.

Table 1 shows some deduced space-filling and non-space-filling lattices suitable for simulations in one dimension. Non-space-filling lattices are always denoted with an 'n'. Some of the lattices found in this work have been found before by other authors. When that is the case, the source is cited in the table. Although one-dimensional problems are very limited and have not great practical usage, the study of these lattices can shed some light on important issues related to the construction of discrete velocity sets by quadrature and on the effect of the inclusion of high order moments in the equilibrium distribution.

One dimensional minimal non-space-filling lattices were found by Chikatamarla and Karlin (2006) using a Gauss-Hermite quadrature. In the same work, these authors reported several different solutions for the problem of finding a lattice with five different velocities, realizing that the lattice formed by the velocities $\{0, \pm1, \pm2\}$ do not have a solution with real and positive weights W_i.

In the present work, the method of prescribed abscissas was applied to find a third order lattice formed by the velocities $\{0, \pm a, \pm b\}$. The results are summarized in the Table 4. The weights and the speed a obtained depend only on the parameter b. They must be non-negative and real if the lattice is valid as a solution of the quadrature problem. Therefore the parameter b is restricted to be larger than or equal to $\sqrt{3+\sqrt{6}}$. The ratio between the two non-zero speeds can be written as $b/a = b\sqrt{(b^2-3)}/\sqrt{3(b^2-5)}$.

Table 1. One dimensional lattices, see Chikatamarla [16] and Tables 4 and 5 for further details.

Moment	Lattices	Moment	Lattices
ξ^2	D1Q3	ξ^6	D1V11, D1V7n
ξ^3	D1V5, D1V4n	ξ^7	D1V13, D1V8n
ξ^4	D1V7, D1V5n	ξ^8	D1V15, D1V9n
ξ^5	D1V9, D1V6n		

This function has a minimum ($b/a \approx 2.107$) when $b = \sqrt{5+\sqrt{10}}$. This means that the ratio between a and b must be at least larger than 2.107 in order to the system have a valuable solution. There are two possible solutions to the quadrature problem when the ratio between the two speeds is smaller than $\sqrt{2}+\sqrt{3}$ and only one possible solution when the ratio is larger than that, Table 4. If the parameter b is chosen so as to retrieve the fourth order moment, the D1V5n lattice is obtained. When the parameter b is chosen so as to make the weight $W_0 = 0$, the D1V4n lattice is obtained [16].

In the Table 2 two dimensional lattices obtained by using the quadrature method with prescribed abscissas are shown, including the references where these lattices were also found by different authors. It can be seen that when the quadrature order is small there is almost no difference between the number of velocities in the space-filling and in the non-space-filling lattices, but when the quadrature order increases, the number of velocities in the non space-filling lattices can be significantly smaller. This tendency is specially prominent in three dimensional sets of velocities, as shown in the Table 3.

Considering two dimensional lattices, although second order sets of velocities, such as the hexagonal lattice, can be built with less than nine directions, they are not of common practical usage, because the D2Q9 lattice is very simple indeed.

Third order lattices can be constructed with twelve velocities without any rest distribution function. These lattices are very simple to handle and can be employed on the simulation of isothermal hydrodynamic problems up to the first Kn order. The D2V12n can be alternatively constructed using a) two sub-lattices with 04-velocities aligned along the main directions and a third one aligned along the diagonals or b) with two sub-lattices aligned along the diagonals and and a third one aligned along the main directions. The solution for the weights and speeds is unique for each one of these lattices.

If a rest distribution function is included in the set of velocities, the system will have a free parameter that can be used to adjust the lattice. In that case, considering, e.g., the first lattice above mentioned, the ratio between the speeds relating the two sub-lattices aligned along the main direction is $b/a = b\sqrt{(b^2-3)}/\sqrt{3(b^2-6)}$.

The free parameter b has restrictions and properties similar to those of the one dimensional D1V5 lattice and the function b/a has a minimum value at $1+\sqrt{2}$. No set of speeds with integer ratios between each other is a possible solution of the quadrature problem, i.e., there is no space-filling lattice with thirteen velocities that retains moments up to the third order using this formulation.

In accordance with a CE analysis, sets of velocities that are able to retrieve all the third order moments and the $\xi^2\xi_\alpha\xi_\beta$ moment can be used to simulate full thermohydrodynamic problems

Table 2. Two dimensional lattices.

Moment	Space-filling	Non-space-filling	
$\xi_\alpha\xi_\beta$	D2Q9 [4,7]	D2Q7n	[4]
$\xi_\alpha\xi_\beta\xi_\gamma$	D2V17 [4,7]	D2V12n	[4,17]
$\xi^2\xi_\alpha\xi_\beta$	D2V25 [7]	D2V17n	Table 6
$\xi_\alpha\xi_\beta\xi_\gamma\xi_\delta$	D2V37 [7]	D2V19n, D2V20n, D2V21n	[17–19], Tables 7–9
$\xi_\alpha\xi_\beta\xi_\gamma\xi_\delta\xi_\epsilon$	D2V53 [8], Table 11	D2V28n	[19], Table 10

Table 3. Three dimensional lattices.

Moment	Space-filling		Non-space-filling	
$\xi_\alpha\xi_\beta$	D3Q15	[4]	D3V13n	[4,19]
$\xi_\alpha\xi_\beta\xi_\gamma$	D3V39	[4,19]	D3V27n	[4,19]
$\xi^2\xi_\alpha\xi_\beta$	D3V59	Table 13	D3V33n	Table 12
$\xi_\alpha\xi_\beta\xi_\gamma\xi_\delta$	D3V107	Table 15	D3V52n, D3V53n	[19,20], Table 14

up to the first Kn order, as the D2V17n lattice. This lattice has a free parameter that could not be applied to lower the number of velocities or increase the number of moments retrieved and mantain all the weights and velocities real and positive at same time, so this free parameter was set to make the set of velocities as compact as possible. The degree of compactness of a lattice is here defined as the ratio between the higher and the lower speeds in the velocity set.

Considering now the LB equation that are built by imposing the orthogonality and norm preservation of all the fourth order equilibrium moments. The smaller velocity set that was found is formed by the zero velocity and three hexagonal sets of velocities. As this lattice is not easy to handle and not symmetric with respect to the x and y axis, other lattices with more velocities were searched. A symmetrical lattice that can be useful is the D2V20n lattice, Table 8. If a rest distribution function is added to this lattice, there is more freedom to choose the shape of the lattice. The D2V21n lattice shown in Table 9 is more compact than the D2V20n lattice, which is important if a algorithm with differents Courant numbers in each direction is used.

Fifth order lattices were also derived in the present work, considering their potential use in problems with high Kn or with two relaxation times [9]. The D2V28n lattice is shown in the Table 10. This lattice is much smaller and compact than the D2V53 lattice, Table 11.

Historically, the most common three-dimensional lattices used in the LB method are the D3Q15 and D3Q19. Although it was found a lattice with thirteen velocities that is suitable to simulate moments up to the second order, this lattice is not easy to handle and has little practical value when compared to the formers.

A fourth order lattice with 33 velocities was found in this work using the prescribed abscissas method [7]. The D3V33n lattice which weights are shown in Table 12, can be a useful lattice for simulating thermohydrodynamic problems. In addition, it is a lattice of very easy practical implementation. Furthermore, the number of velocities is significantly lower than its space-filling counterpart (the D3V59 lattice, Table 13) and the 77-velocities lattice proposed by Watari [11].

In order to recover all the moments up to the fourth order, a space-filling lattice composed by 107 velocities have to be constructed, Table 15. This velocity set is computational expensive and requires to improve the boundary conditions rules for assuring non-slip and temperature continuity at the solid surfaces that bound the flow domain. Its non-space-filling lattice counterpart, a lattice composed by 52 velocities, Table 3, halves the memory occupied and, considering methods that involves the derivative calculation based only on the information of the two nearest neighbours, this lattice does not increases the complexity of the algorithm used. Nevertheless, the D3V52n lattice is not compact, i.e., the ratio between the lower non-zero speed and the higher speed equals ≈ 7.518. The D3V53n, in contrast, is much more compact, e.g., the ratio between the lower and the higher speed is ≈ 3.317.

3 Results

A finite difference scheme was used for the streaming term of the continuous Boltzmann equation, trying to reduce the errors related to the mesh spacing dx and time step dt. Therefore, the discretization of the time derivative was performed using a second order Runge-Kutta scheme and the spatial derivative was calculated with a third order upwind scheme using points aligned with the direction of the velocity $\boldsymbol{\xi}_i$ whenever there were points of the spatial mesh along this same direction. When that was not the case, an interpolation scheme was used considering the points that were nearest to the $\boldsymbol{\xi}_i$ direction. For writing the boundary conditions, the distributions f_i were expanded in Hermite polynomials up to the quadrature order N splitting this expansion into an equilibrium and a non-equilibrium part:

$$f_i = f_i^{eq} + f_i^{neq} = \sum_{n=0}^{N} \frac{1}{n!} a_n^{eq}(\rho, u_\alpha, T)\mathscr{H}_n(\boldsymbol{\xi}_{oi}) + \sum_{n=2}^{\infty} \frac{1}{n!} a_n^{neq}(\tau_{\alpha\beta}, q_\alpha, \ldots)\mathscr{H}_n(\boldsymbol{\xi}_{oi}). \tag{4}$$

The known moments on the boundary, i.e., the velocity and the temperature, were imposed for establishing the coefficients a_n^{eq}. The non-equilibrium-moments and the density were approximated by an extrapolation from the nearby fluid sites, see [3].

Although this scheme has an important drawback since it is impossible to warrant the mass preservation, the error that was found in the simulations was below 1% in the most of the sample cases that were analyzed.

3.1 Sod's shock tube

The Sod's shock tube problem [14], was simulated for comparing some of the one dimensional lattices exposed in Section 2 (D1V4n, D1V5n, D1V7n and D1V9n). The main purpose was to evaluate the effect of including higher order moments in the discrete equilibrium distribution function and the effect of the temporal and spatial discretization in the solution.

The Sod's shock tube problem consists in a domain with a diaphragm separating a region of high pressure, where the density equals 8 and temperature equals 1.00, on the left from a region of low pressure, density equals 1 and temperature equals 0.75, on the right. When the diaphragma is broken a compression wave propagates to the right and an expansion wave propagates to the left. The pressure ratio between the two sides equals 10.

The Figure 1(a) shows the pressure distribution in two different simulations, using two different temporal-spatial discretizations: the first discretization, which results are shown in Figures 1(a), 1(b) and 1(c), is four times coarser than the second one, shown in Figures 1(d), 1(e) and 1(f).

In the Figure 1(a) some instabilities can be observed, what can be caused either by the spatial and temporal discretization or the failure of representing correctly the equilibrium distribution and the velocity space discretization associated with this. Analysing the expansion wave with details, 1, it can be observed that all the velocity space discretizations, from the third to the eighth order, presented the same results, suggesting that what causes the instabilities is not the velocity space discretization. When the time and spatial steps were diminished, Figure 1(e), this expectation was confirmed by the disappearing of the instabilities, both in the expansion and in the compression waves, compare Figure 1(c) and Figure 1(f). The difference between the ideal gas solution and the Boltzmann equation solution is due both to physical aspects, i.e., heat diffusion and high Kn effects, and to errors of the algorithm, i.e., numerical diffusion. Nevertheless, the results are in very good agreement with each other and the algorithm is very stable up to pressure ratios of fifty, as long as the temperature is lowered, the thermal diffusivity is increased to avoid instabilities and the time step is diminished.

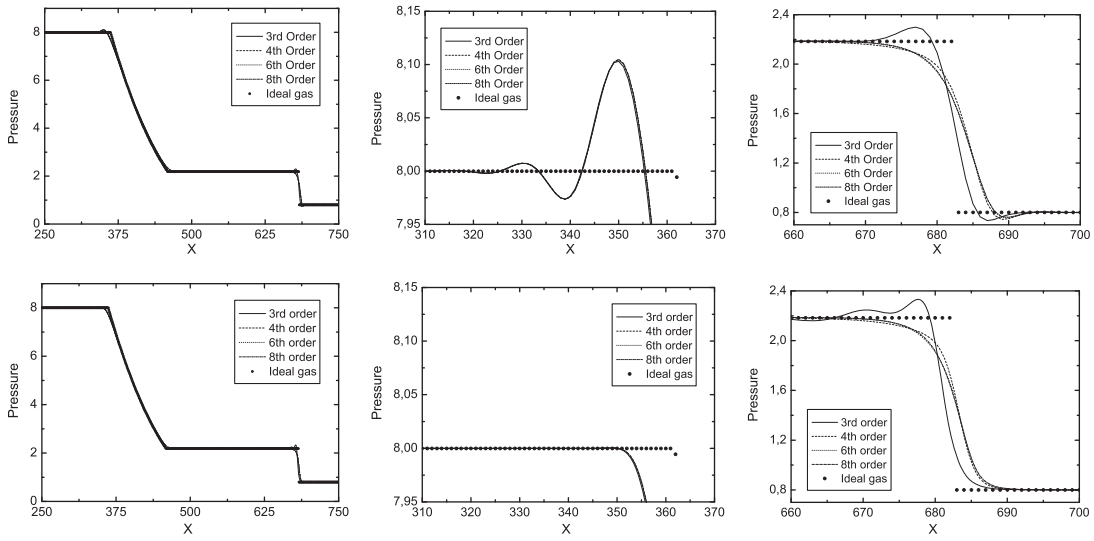

Fig. 1. Sod's shock tube.

It can be also observed that the D1V4n is not able to simulate this problem due essentially to the inexact calculation of the fourth order moments, which is a necessary condition to represent all the thermohydrodynamics up to the first Kn order [7].

3.2 Couette flow

Using the boundary conditions that were described in the beginning of Section 3, the Couette flow between two infinite plates at different temperatures and velocities were simulated using the D2V17n lattice. The Eckert number is given by $E_c = U^2/c_v \Delta T$, where U is the velocity on the east wall, c_v is the constant volume specific-heat and ΔT is the temperature difference between the walls. The velocity was set to zero on the west wall and, in accordance with the Eckert number, different from zero on the east wall. On the west wall the temperature was set to 0.99 and on the east one to 1.01. The simulations were performed using Eckert numbers from 1 to 32 and the results are summarized on Figure 2(a) and 2(b). There is a very good agreement with the exact solutions for all the Eckert numbers tested, even when the number of points in the mesh is very low and the Mach number is high. No velocity slip or temperature jump were reported.

3.3 Lid-driven cavity flow

In the lid-driven cavity flow a non-zero velocity is imposed on the top surface of a closed square cavity. Simulations were performed using the D2V17n lattice and an isothermal equilibrium distribution. The purpose was to find the stability limits of the method and its ability to simulate this hydrodynamic problem. The Figures 3(a) and 3(b) show the $u_x(x = 0.5, y)$ component along the median axis $x = 0.5$ and the $u_y(x, y = 0.5)$ component along the median axis $y = 0.5$, when the Reynolds number is 1000.

Although these results are to be considered as very good when compared with the work of Ghia et al. [21], they have only been obtained with a small mesh size, and, consequently, with a very small time-step, requiring a significantly high number of time steps until convergence.

In the LB method collision-propagation simulation there is always an anti-diffusive effect brought out by the factor $-\delta/2$ [22]. This effect is absorbed into the viscosity and thermal diffusivity, enabling the simulation of the same Reynolds number flows with larger time steps when compared with present high-order finite difference scheme, since the over-relaxation of the collision term leads to viscosities that can be very low when compared with the present ones.

4 Conclusions

In this work, non-space-filling lattices suitable for solving the Boltzmann equation using finite diference and, although not tested, finite element and finite volume methods were derived using

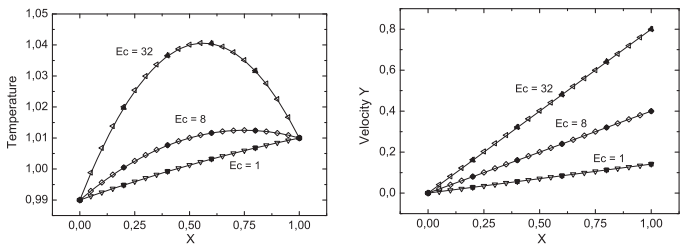

Fig. 2. Couette flow. The temperature a) and velocity b) are compared with the Navier-Stokes-Fourier equation solution. The simulation results are the dots and the lines are the analytical solutions.

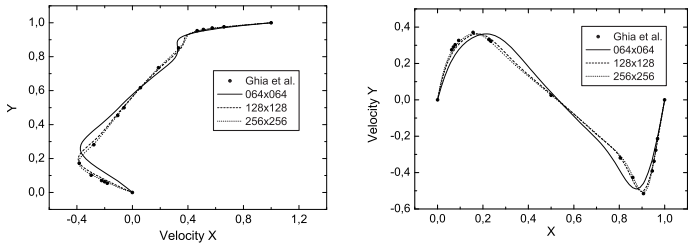

Fig. 3. Lid-driven cavity flow, Re = 1000.

the quadrature based on prescribed abscissas. The sets of velocities found are smaller and more compact than theirs space-filling counterparts, what can be specially important when more equilibrium distribution moments must be retrieved and tridimensional lattices are used.

Although the lattices found proved to be able to simulate the complete set of equations of the thermohydrodynamics up to the Navier-Stokes level, more tests with tridimensional lattices, adaptative meshes, different algorithms and different boundary conditions are still on course and will be reported elsewhere. The numerical diffusion seems to be a great problem when finite difference schemes are used, limiting the application of these methods to large domains.

The authors want to acknowledge the support provided by the CNPq (The National Council for Scientific and Technological Development), Finep (Research and Projects Financing) and Petrobras (Petróleo Brasileiro S/A).

A Lattices

Table 4. Possible choices for D1V5.

	W_0	W_1	W_2	a
$\{0, \pm a, \pm 2a\}$	no solution			
$\{0, \pm a, \pm 3a\}$	7.446420×10^{-2}	4.185854×10^{-1}	4.418248×10^{-2}	7.826711×10^{-1}
$\{0, \pm a, \pm 3a\}$	6.366469×10^{-1}	1.814146×10^{-1}	2.619607×10^{-4}	1.649472
$\{0, \pm a, \pm 4a\}$	6.513812×10^{-1}	1.742737×10^{-1}	3.575170×10^{-5}	1.691054
$\{0, \pm a, \pm b\}$	$\frac{2(b^4-6b^2+3)}{3b^2(b^2-5)}$	$\frac{(b^2-3)^3}{6(b^6-11b^4+45b^2-75)}$	$\frac{3}{b^2(b^4-6b^2+15)}$	$\sqrt{3+\frac{6}{3-b^2}}$

Table 5. One dimensional lattices.

	D1V7	D1V9	D1V11	D1V13	D1V15
c_s	1.447018	2.554632	1.785604	2.832466	2.069553
W_0	4.766699×10^{-1}	1.672402×10^{-1}	3.869382×10^{-1}	2.092777×10^{-1}	3.338809×10^{-1}
W_1	2.339147×10^{-1}	3.031542×10^{-1}	2.417834×10^{-1}	2.331246×10^{-1}	2.352338×10^{-1}
W_2	2.693819×10^{-2}	5.330294×10^{-2}	5.892246×10^{-2}	9.405107×10^{-2}	8.226164×10^{-2}
W_3	8.121295×10^{-4}	5.792153×10^{-2}	5.615255×10^{-3}	5.692338×10^{-2}	1.428014×10^{-2}
W_4			2.065248×10^{-4}	7.500768×10^{-3}	1.230146×10^{-3}
W_5		2.001260×10^{-3}	3.274472×10^{-6}	3.700559×10^{-3}	5.267663×10^{-5}
W_6					1.106671×10^{-6}
W_7				6.078434×10^{-5}	1.294923×10^{-8}

Table 6. D2V17n.

$\boldsymbol{\xi}_i$	i	W_i
$(0,0)$	1	$2.91120705068934 \times 10^{-1}$
$(\pm a,0)$	4	$1.17544259079499 \times 10^{-1}$
$(\pm a,\pm a)$	4	$4.99848074155116 \times 10^{-2}$
$(\pm b,0)$	4	$7.38568353112397 \times 10^{-3}$
$(\pm c,\pm c)$	4	$2.30507370663218 \times 10^{-3}$

$a = 1.36967763379$
$b = 2.98493018050$
$c = 2.38098279882.$

Table 7. D2V19n.

$\boldsymbol{\xi}_i$	i	W_i
$(0,0)$	1	$\frac{31}{96}$
$a(sin(\pi i/3), cos(\pi i/3))$	6	$\frac{605+151\sqrt{15}}{11520}$
$b(sin(\pi i/3+\pi/6), cos(\pi i/3+\pi/6))$	6	$\frac{1}{128}$
$c(sin(\pi i/3), cos(\pi i/3))$	6	$\frac{605-151\sqrt{15}}{11520}$

$a = 2\sqrt{\frac{2}{7}\left(6-\sqrt{15}\right)}$, $b = 2\sqrt{2}$, $c = 2\sqrt{\frac{2}{7}\left(6+\sqrt{15}\right)}$.

Table 8. D2V20n.

$\boldsymbol{\xi}_i$	i	W_i
$(\pm a,\pm a)$	4	$1.88925845284202 \times 10^{-1}$
$(\pm b,0)$	4	$3.93820098682627 \times 10^{-2}$
$(\pm c,\pm c)$	4	$2.08333333333333 \times 10^{-2}$
$(\pm d,\pm e)$	8	$4.29405757101158 \times 10^{-4}$

$a = 0.68125003863$ $\quad d = 1.3665853546$
$b = 2.17532774716$ $\quad e = 3.6873494659.$
$c = 1.73205080757$

Table 9. D2V21n.

$\boldsymbol{\xi}_i$	i	W_i
$(0,0)$	1	$2.05660006833783 \times 10^{-1}$
$(\pm a,\pm a)$	8	$1.40509662171466 \times 10^{-1}$
$(\pm b,0)$	4	$4.38226426701393 \times 10^{-2}$
$(\pm c,\pm c)$	4	$1.24095396776270 \times 10^{-2}$
$(\pm 3d,\pm d)$	8	$9.21576886161059 \times 10^{-4}$

$a = 0.84919384991$ $\quad c = 1.8616199350$
$b = 2.06813606112$ $\quad d = 1.1386549808.$

Table 10. D2V28n.

$\boldsymbol{\xi}_i$	i	W_i
$(\pm a,\pm a)$	4	$1.65178143204339 \times 10^{-1}$
$(\pm b,0)$	4	$4.76436948919026 \times 10^{-2}$
$(\pm c,\pm c)$	4	$3.13893609813488 \times 10^{-2}$
$(\pm 2d,\pm d)$	8	$2.60416666666667 \times 10^{-3}$
$(\pm e,0)$	4	$5.66775193567500 \times 10^{-4}$
$(\pm f,\pm f)$	4	$1.36923955088259 \times 10^{-5}$

$a = 0.60908304548$ $\quad d = 1.4142135623$
$b = 1.96450120032$ $\quad e = 3.6707040697$
$c = 1.45841718745$ $\quad f = 3.4441308266.$

Table 11. D2V53, $a = 1.12787327020759509$.

$\boldsymbol{\xi}_i$	i	W_i
$(0,0)$	1	$2.05255299930058 \times 10^{-1}$
$(\pm a,0)$	4	$1.04840518201578 \times 10^{-1}$
$(\pm a,\pm a)$	4	$5.86865864166755 \times 10^{-2}$
$(\pm 2a,0)$	4	$1.67906473563003 \times 10^{-2}$
$(\pm 2a,\pm a)$	8	$7.65724340287832 \times 10^{-3}$
$(\pm 2a,\pm 2a)$	4	$1.54868631971367 \times 10^{-3}$
$(\pm 3a,0)$	4	$5.24980317084264 \times 10^{-4}$
$(\pm 3a,\pm a)$	8	$4.77912601004212 \times 10^{-4}$
$(\pm 4a,\pm a)$	8	$6.07479146296177 \times 10^{-6}$
$(\pm 3a,\pm 3a)$	4	$1.19642275835789 \times 10^{-5}$
$(\pm 5a,0)$	4	$3.30587859576316 \times 10^{-7}$

Table 12. D3V33n.

$\boldsymbol{\xi}_i$	i	W_i
$(0,0,0)$	1	$1.69544317872168 \times 10^{-1}$
$(\pm a,0,0)$	6	$7.53752058968985 \times 10^{-2}$
$(\pm b,\pm b,\pm b)$	8	$3.90045337112442 \times 10^{-2}$
$(\pm c,0,0)$	6	$6.86518217744201 \times 10^{-3}$
$(\pm d,\pm d,0)$	12	$2.08142366598628 \times 10^{-3}$

$a = 1.07182071542885$ $\quad c = 2.92338002226218$
$b = 1.21422495340964$ $\quad d = 2.49326392161601.$

Table 13. D3V59, $a = 1.20288512331026$.

$\boldsymbol{\xi}_i$	i	W_i
$(0,0,0)$	1	$9.58789162377528 \times 10^{-2}$
$(\pm a,0,0)$	6	$7.31047082129148 \times 10^{-2}$
$(\pm a,\pm a,0)$	12	$3.46588971093380 \times 10^{-3}$
$(\pm a,\pm a,\pm a)$	8	$3.66108082044515 \times 10^{-2}$
$(\pm 2a,0,0)$	6	$1.59235232232060 \times 10^{-2}$
$(\pm 2a,\pm 2a,0)$	12	$2.52480845105094 \times 10^{-3}$
$(\pm 2a,\pm 2a,\pm 2a)$	8	$7.26968662515159 \times 10^{-5}$
$(\pm 3a,0,0)$	6	$7.65879439346840 \times 10^{-4}$

Table 14. D3V53n.

$\boldsymbol{\xi}_i$	i	W_i
$(0,0,0)$	1	$1.60453547343974 \times 10^{-1}$
$(\pm a,0,0)$	6	$7.17493485726724 \times 10^{-2}$
$(\pm b,\pm b,\pm b)$	8	$3.85210759331158 \times 10^{-2}$
$(\pm c,\pm d,0)$	24	$4.11522633744856 \times 10^{-3}$
$(\pm e,\pm e,\pm e)$	8	$2.44958972443801 \times 10^{-4}$
$(\pm f,0,0)$	6	$2.61083127915713 \times 10^{-5}$

$a = 1.45239166695403$ $d = 2.66422150193135$
$b = 1.12267801869052$ $e = 2.40894358132745$
$c = 1.37910253014295$ $f = 4.81788716265490.$

Table 15. D3V107, $a = 1.07182071542885$.

$\boldsymbol{\xi}_i$	i	W_i
$(0,0,0)$	1	$7.57516860965017 \times 10^{-2}$
$(\pm a,0,0)$	6	$6.00912802747447 \times 10^{-2}$
$(\pm a,\pm a,0)$	12	$3.13606906699535 \times 10^{-3}$
$(\pm a,\pm a,\pm a)$	8	$3.63392812078012 \times 10^{-2}$
$(\pm 2a,0,0)$	6	$1.32169332731492 \times 10^{-2}$
$(\pm 2a,\pm a,0)$	24	$4.48492851172950 \times 10^{-3}$
$(\pm 2a,\pm 2a,0)$	12	$2.48755775808342 \times 10^{-3}$
$(\pm 3a,\pm a,\pm a)$	24	$6.07432754970149 \times 10^{-4}$
$(\pm 2a,\pm 2a,\pm 2a)$	8	$4.64179164402822 \times 10^{-4}$
$(\pm 4a,0,0)$	6	$4.51928894609872 \times 10^{-5}$

References

1. Y.H. Qian, D. d'Humières, P. Lallemand, Europhys. Lett. **17**, 479 (1992)
2. P.L. Bhatnagar, E.P. Gross, M. Krook, Phys. Rev. **94**, 511 (1954)
3. G. McNamara, B. Alder, Physica A **194**, 218 (1993)
4. X. Shan, X. Yuan, H. Chen, J. Fluid Mech. **550**, 413 (2006)
5. F.J. Alexander, S. Chen, J.D. Sterling, Phys. Rev. E **47**, R2249 (1993)
6. Y. Chen, H. Ohashi, M. Akiyama, Phys. Rev. E **50**, 2776 (1994)
7. P.C. Philippi, L.A. Hegele Jr., L.O.E. dos Santos, R. Surmas, Phys. Rev. E **73**, 056702 (2006)
8. P.C. Philippi, L.A. Hegele Jr., R. Surmas, D.N. Siebert, L.O.E. dos Santos, Int. J. Mod. Phys. C **18**, 556 (2007)
9. D.N. Siebert, L.A. Hegele Jr., R. Surmas, L.O.E. dos Santos, P.C. Philippi, Int. J. Mod. Phys. C **18**, 546 (2007)
10. P. Pavlo, G. Vahala, L. Vahala, Phys. Rev. Lett. **80**, 3960 (1998)
11. M. Watari, M. Tsutahara, Phys. Rev. E **70**, 016703 (2004)
12. C.E. Pico, L.O.E. dos Santos, P.C. Philippi, Int. J. Mod. Phys. C **18**, 566 (2007)
13. R. Cools, J. Complex. **19**, 445 (2003)
14. G.A. Sod, J. Comput. Phys. **27**, 1 (1978)
15. C. Cercignani, *The Boltzmann Equation and Its Applications* (Springer-Verlag, New York, 1988)
16. S.S. Chikatamarla, I.V. Karlin, Phys. Rev. Lett. **97**, 190601 (2006)
17. A.H. Stroud, *Approximate Calculation of Multiple Integrals* (Prentice-Hall, Englewood Cliffs, 1971)
18. A. Haegemans, *Tables of circularly symmetrical integration formulas of degree 2d-1 for two - dimensional circulatory symmetrical regions* (Report TW 27, K.U. Leuven Applied Mathematics and Programming Division, 1975)
19. C.E. Pico, *Aplicação das formas discretas da equação de Boltzmann à termo-hidrodinâmica de misturas*, Ph.D. thesis, UFSC, Florianópolis, 2007
20. F. Mantel, P. Rabinowitz, SIAM J. Numer. Anal. **14**, 391 (1977)
21. U. Ghia, K.N. Ghia, C.T. Shin, J. Comput. Phys. **48**, 387 (1982)
22. V. Sofonea, R.F. Sekerka, J. Comput. Phys. **184**, 422 (2003)